In Situ Generated Heterometallic Nickel-Zinc Catalysts for Ethylene Polymerization

Dawei Xiao, Loi H. Do*

Department of Chemistry, University of Houston, 4800 Calhoun Rd., Houston, TX 77004, United States

Supporting Information Placeholder

ABSTRACT: We have prepared a new series of organometallic nickel complexes ligated by 1-picolyl-4-carboxamidate-1,2,3-triazole donors. Solution metal binding studies by NMR spectroscopy indicated that their reactions with zinc chloride led to the formation of nickel-zinc heterometallics with undefined compositions. These nickel-zinc complexes showed increasing ethylene polymerization activity over the course of 3 h and provided polymers with multimodal distributions. In comparison, the mononickel complexes exhibited constant activity over time and gave narrowly dispersed low molecular weight polyethylene (M_n = ~10^3). The addition of zinc sources other than $ZnCl_2$ or other metal salts to the mononickel catalysts did not lead to enhancements in their catalytic performance. Our results suggest that further modifications of the carboxamidatetriazole platform are needed to obtain well-defined heterobimetallic complexes for the controlled synthesis of ethylene-based polymers.

INTRODUCTION

Biological enzymes often utilize multi-metallic centers to activate or orient substrates in complex chemical reactions.[1] Chemists have long sought to mimic such cooperative reactivity in synthetic catalysts with varying degrees of success. For example, multi-metallic complexes have been explored for their ability to assist in olefin polymerization catalysis.[2-5] It is proposed that the various metal sites in polynuclear catalysts could play different roles in the polymerization process, such as favoring one insertion pathway over another, providing alternative binding sites for polar monomers,[6,7] or accelerating the reaction kinetics.[8,9]

Heterobimetallic complexes are particularly attractive as olefin polymerization catalysts because they could access reactivity patterns that are inaccessible using their homobimetallic counterparts.[2] A variety of dinucleating ligands have been used to prepare heterobimetallics, which differ in their metal binding affinities and M–M bond distances when metallated. For example, Johnson/Brookhart and coworkers have reported a nickel phosphine alkoxide catalyst that could coordinate lithium ions (Type I, Chart 1).[10] It was shown that ancillary donor groups are required to kinetically stabilize Li^+ within the ligand framework. In another example, Osakada and coworkers utilized an organic spacer to link together an early metal zirconium oligomerization catalyst with a late metal nickel polymerization catalyst (Type II).[11] Due to its long zirconium-nickel separation, this complex cannot engage in any direct metal-metal interactions. In a third example, Tonks and coworkers took advantage of 2,6-bis(imino)phenoxide ligands to assemble nickel-zinc heterobimetallics (Type III).[12] Because the phenoxide group bridges both nickel and zinc, the two metal centers are in close contact. There are many other heterobimetallics that fall within one of these three groups, although other structural types are also known.[13-16]

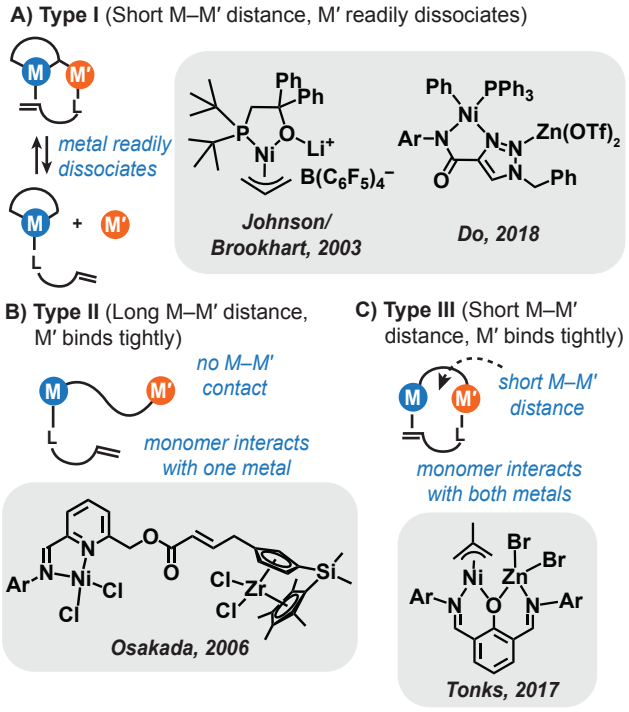

Chart 1. Various dinucleating ligands used to prepare heterobimetallic catalysts for olefin polymerization. Select examples are provided to showcase their heterobimetallic structures.

Deciding which types of heterobimetallic complexes to employ in polymerization reactions depend on their applications.[2] In our laboratory, we are primarily interested in those where both metal centers could engage cooperatively with functional monomers such as acrylates, vinyl ethers, or allyl acetates. Our

goal is to introduce new reaction pathways to avoid unfavorable coordination isomerization and polar group chelation that is believed to hinder coordination-insertion processes.[17-19] To achieve this objective, we will take advantage of type III heterobimetallics that are kinetically stable and have short metal-metal bond distances. In a previous study, we devised a new ligand platform based on the 4-carboxamidate-1,2,3-triazole group to prepare the corresponding mononickel complexes (**5**, Chart 1A and Scheme 1).[20] We showed that these Ni species are competent catalysts for ethylene polymerization and could bind external zinc ions. Unfortunately, the addition of zinc salts to our nickel complexes led to catalyst inhibition in some cases. In the present work, we have appended a picolyl donor to the carboxamidatetriazole ligand to assist in zinc chelation. Surprisingly, our polymerization studies indicated that the nickel-zinc species derived from this modified ligand were not single-site catalysts. These investigations underscore the pitfalls commonly encountered in new catalyst development and the importance of undertaking an iterative design process to create suitable supporting ligands.

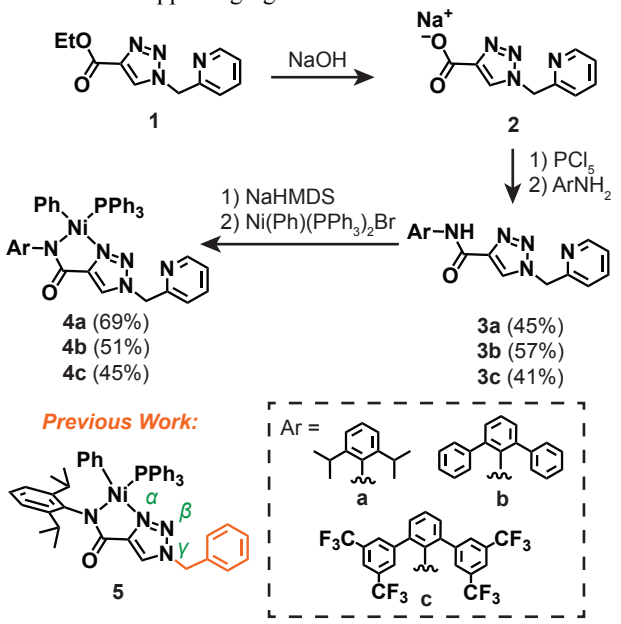

Scheme 1. Synthesis of complexes **4a**-**4c** and the structure of **5** for comparison.

RESULTS AND DISCUSSION

Synthesis and Characterization of Nickel Complexes. Although our first-generation nickel carboxamidatetriazole complex **5** (Scheme 1) showed promising ethylene polymerization behavior, the addition of zinc salts did not lead to any beneficial heterobimetallic effects.[20] We hypothesized that perhaps Zn^{2+} was dissociating too readily from **5** or that the nickel-zinc species did not have optimal active sites for polymerization.

To improve zinc chelation by the nickel carboxamidatetriazole catalysts, we introduced picolyl donors to the γ-positions of their triazole rings. The synthetic sequence to obtain our second-generation catalysts is shown in Scheme 1. First, the copper-catalyzed click reaction between 2-picolyl azide and propargylic ethyl ester provided compound **1** in moderate yields.[21] The ester group in **1** was hydrolyzed using sodium hydroxide and then converted to the acyl chloride by treatment with PCl_5. Subsequent reactions with an arylamine furnished the desired ligands in high purity after workup. We prepared three ligand derivatives that differ in their steric bulk, specifically those containing 2,6-bis(isopropyl)phenyl (**3a**), 2,6-bis(phenyl)phenyl (**3b**),[22] and 2,6-bis(3,5-bis(trifluoromethyl)phenyl)phenyl (**3c**)[22] *N*-amide substituents. The nickel complexes **4a**-**4c** were synthesized by reacting the corresponding deprotonated ligands with $Ni(Ph)(PPh_3)_2Br$[23] to afford the desired products as yellow solids (45-69% yield).

Crystallization of complex **4a** from a mixture of dichloromethane and pentane gave yellow blocks suitable for X-ray diffraction analysis. As shown in Figure 1, complex **4a** adopts a square planar arrangement, similar to that in our previous nickel complexes.[20] The phosphine group (Ni–P = 2.17 Å) is ligated *trans* relative to the anionic carboxamidate moiety (Ni–N = 1.95 Å). As expected, the picolyl group is not coordinated in this structure but based on studies by Bai et. al., the triazole-picolyl unit is a good chelator for copper and zinc ions.[24]

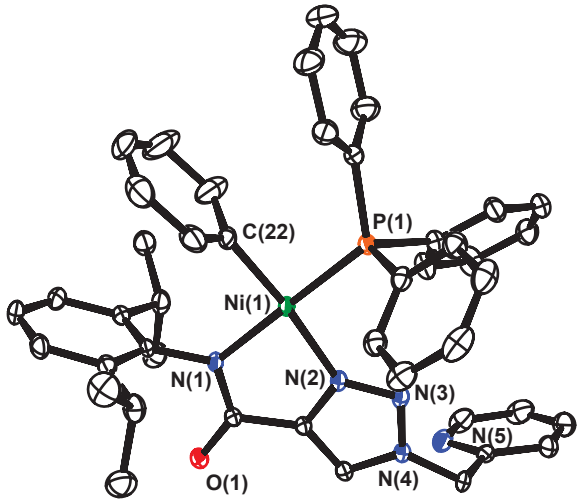

Figure 1. X-ray crystal structure of Ni(**3a**)(Ph)(PPh_3) (**4a**, ORTEP view, displacement ellipsoids drawn at 50% probably level). Hydrogen atoms and solvent molecules have been omitted for clarity. Bond lengths (Å): Ni(1)–N(1) = 1.970, Ni(1)–N(2) = 1.946, Ni(1)–C(22) = 1.885, and Ni(1)–P(1) = 2.171. Bond angles (°): N(1)–Ni(1)–C(22) = 91.9, C(22)–Ni(1)–P(1) = 88.1, P(1)–Ni(1)–N(2) = 97.3, and N(1)–Ni(1)–N(2) = 82.4.

Secondary Metal Ion Binding. The coordination chemistry of our nickel compounds was studied by solution NMR spectroscopy. When various equivalents of $ZnCl_2$ were combined with **4a**, **4b**, or **4c** in the non-coordinating solvent $CDCl_3$, the mixtures all showed changes in their ^1H NMR spectra (Figures S18, S22-S23). In general, the addition of increasing amounts of zinc ions led to greater peak broadening, which suggests that there might be dynamic exchange of Zn^{2+} ions in solution or multiple nickel-zinc species are interconverting. To probe their solution behavior in more detail, we carried out variable temperature studies of **4c** and **4c**/$ZnCl_2$ (1:1). When the solution temperature was lowered from 25°C to 0°C, the triazole proton resonance at ~7.8 ppm (peak *f*, Figure 2) could not be observed. However, upon further cooling to -50°C, the triazole peak reappeared at a similar chemical shift. Peak broadening also occurred in the ^{13}C (Figure S25) and ^{31}P (Figure S26) NMR spectra of **4c**/$ZnCl_2$ compared to those of **4c** only. Since the ^{31}P NMR signal at ~31 ppm does not shift

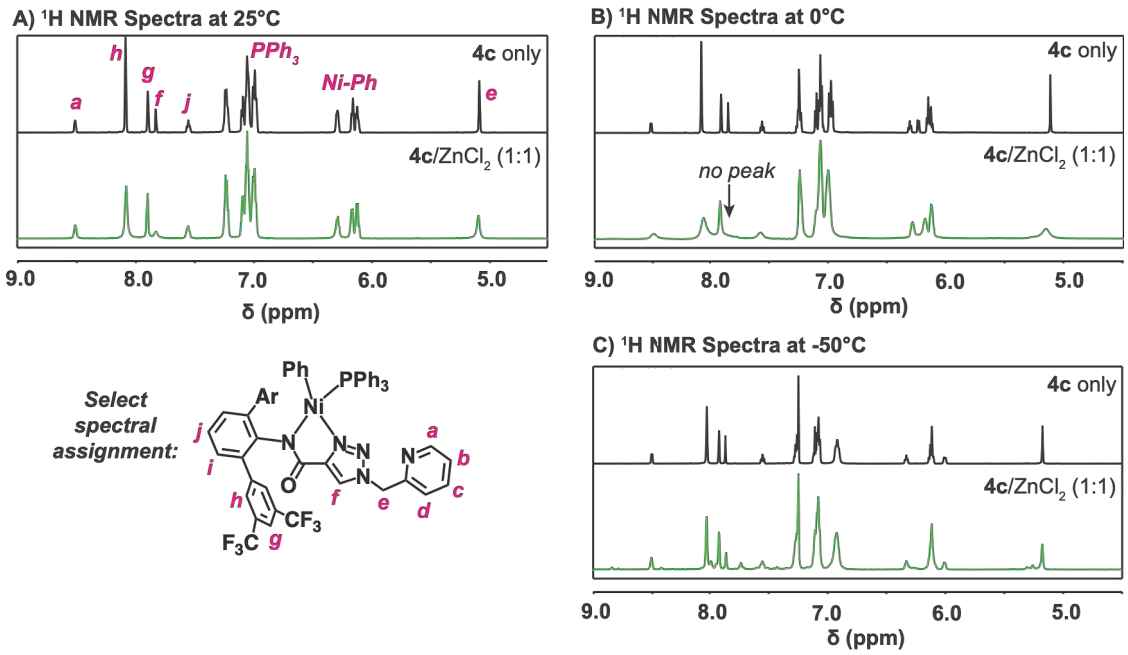

Figure 2. Variable temperature ^{1}H NMR spectra ($CDCl_3$, 600 MHz) of complexes **4c** and **4**c/$ZnCl_2$ (1:1) shown as stacked plots for comparison. Select peak assignments (*a*-*j*) are provided in the structure above for **4c**.

appreciably in **4c** vs. **4c**/$ZnCl_2$, it appears that the presence of zinc does not alter the primary coordination sphere of the nickel center. Despite many attempts, we were unable to grow single crystals of the nickel-zinc complexes for structural analysis by X-ray crystallography.

We also studied nickel-zinc binding by UV-vis absorption spectroscopy. When complex **4a** in CH_2Cl_2 was treated with up to 10 equiv. of $ZnCl_2$ (pre-dissolved in EtOH), the absorption feature at ~320 nm shifted to ~330 nm concomitant with a decrease in intensity (Figure S21). The lack of isosbestic points and the inability of the data to fit any simple binding model suggests that the nickel/zinc reaction most likely gives a mixture of products, which would preclude further Job Plot studies. Unfortunately, based on our current characterization data, we are unable to determine the nuclearity or composition of the nickel-zinc products.

Ethylene Polymerization. Our parent nickel complexes **4a**–**4c** were tested as potential catalysts for ethylene polymerization (Table 1). The reactions were carried out using glass reactors at 100 psi of ethylene in the presence of the nickel complexes and the phosphine scavenger $Ni(COD)_2$ (COD = 1,5-cyclooctadiene) at RT for 1 h (entries 1,7, and 11) and 3 h (2, 8, and 12). The turnover frequencies (TOFs) were calculated to be 51, 17, and 19 h^{-1}, respectively, after 1 h and remained relatively constant up to 3 h. In comparison to **5** (TOF = 290 h^{-1}), the catalyst activities of **4a**–**4c** were several times lower, suggesting that the free picolyl groups in the latter structures might be catalyst inhibiting due to intermolecular metal coordination. Catalyst **4a** furnished polyethylene (PE) with higher molecular weight (M_n = 2.80×10^3) than **4b** and **4c** (M_n = 0.51×10^3 and 0.58×10^3, respectively), which is surprisingly because bulkier catalysts typically provide longer polymer chains than their less bulk variants.[25] However, all three catalysts gave narrowly dispersed PE (M_w/M_n = 1.2–1.7) with ~100 branches per 1000 carbon atoms. The PE obtained using **4a** comprised about 78% C_1, 6% C_2, 2% C_3, and 14% C_{4+} branches (Figure S29), which is similar to the PE obtained using complex **5**.[20]

To study the effects of secondary metal ions on ethylene polymerization, we tested catalysts **4a**–**4c** in the presence of various zinc salts (Table 1).[12] We found that the addition of 2 equiv. of $ZnCl_2$, relative to nickel, enhanced the activity of **4a** by ~5.1× (entries 1 vs. 4) and **4b** by ~3.2× (entries 7 vs. 9) compared to their corresponding mononickel catalysts. Using greater than 2 equiv. of zinc salt did not accelerate the polymerization rates any further but did lead to reduction in the polymer molecular weight, which is most likely due to the chain transfer propensity of zinc.[26,27] The addition of $ZnCl_2$ to **4c** gave nearly no product (entry 13), perhaps due to the formation of **4c**/$ZnCl_2$ species that are too sterically hindered to promote polymerization. The application of zinc salts other than $ZnCl_2$, such as $ZnBr_2$, ZnI_2, or $Zn(OSO_2CF_3)_2$, to **4a** had minimal effect on the catalyst activity (Table S1), which was surprising because all of the different zinc salts appeared to bind **4a** in a similar manner (Figure S19). This result suggests that the chloride anions in $ZnCl_2$, but not bromide, iodide, or triflate, are functionally important in the nickel-zinc catalyst structures. Finally, the reaction of **5**/$ZnCl_2$ with ethylene did not show any activity enhancement compared to reactions using just **5** (Table 1, entries 14 vs. 15).

Table 1. Ethylene Polymerization Using Complexes **4** and **5** with $ZnCl_2$[a]

Entry	Cat.	Time (h)	Zinc Salt (equiv.)	Polymer Yield (mg)	TOF (h^{-1})	Branches[b] (/1000 C)	M_n[c] ($\times 10^3$)	M_w/M_n[c]
1	**4a**	1	none	36	51	92	2.99	1.4
2	**4a**	3	none	175	83	96	2.80	1.4
3	**4a**	1	$ZnCl_2$ (1)	59	84	89	2.10	7.6[d]
4	**4a**	1	$ZnCl_2$ (2)	183	261	65	2.01	20.7[d]
5	**4a**	1	$ZnCl_2$ (5)	67	96	52	1.73	24.4[d]
6	**4a**	1	$ZnCl_2$ (10)	74	106	68	0.23	80.6[d]
7	**4b**	1	none	12	17	-	-	-
8	**4b**	3	none	44	21	98	0.51	1.2
9	**4b**	1	$ZnCl_2$ (2)	38	54	53	1.19	51.7[d]
10	**4b**	3	$ZnCl_2$ (2)	194	92	45	6.82	13.5[d]
11	**4c**	1	none	13	19	-	-	-
12	**4c**	3	none	52	25	104	0.58	1.7
13	**4c**	1	$ZnCl_2$ (2)	trace	0	-	-	-
14	**5**	1	none	203	290	101	4.82	2.3
15	**5**	1	$ZnCl_2$ (2)	180	257	95	0.88	2.5

[a]Polymerization conditions: nickel precatalyst (25 μmol), $Ni(COD)_2$ (50 μmol), $ZnCl_2$ (various equiv., if any), ethylene (100 psi), 10 mL toluene, at RT. [b]The total number of branches per 1000 carbons was determined by ^1H NMR spectroscopy. [c]Determined by GPC in trichlorobenzene at 150°C. [d]Multimodal PE distributions.

Table 2. Time Study of Ethylene Polymerization Using **4a** with $ZnCl_2$[a]

Entry	Time (h)	Zinc Salt (equiv.)	Polymer Yield (mg)	TOF (h^{-1})	Branches[b] (/1000 C)	M_n[c] ($\times 10^3$)	M_w/M_n[c]
1	0.5	none	22	63	-	-	-
2	1	none	36	51	97	2.99	1.4
3	2	none	77	55	98	2.62	1.4
4	3	none	175	83	96	2.80	1.4
5	0.5	$ZnCl_2$ (2)	92	263	69	1.06	36.2[d]
6	1	$ZnCl_2$ (2)	184	263	65	2.01	20.7[d]
7	2	$ZnCl_2$ (2)	553	395	28	6.02	13.9[d]
8	3	$ZnCl_2$ (2)	1220	581	34	34.87	6.4[d]
9	6	$ZnCl_2$ (2)	1830	436	36	48.68	4.8[d]

[a]Polymerization conditions: nickel precatalyst (25 μmol), $Ni(COD)_2$ (50 μmol), $ZnCl_2$ (2 equiv., if any), ethylene (100 psi), 10 mL toluene, at RT. [b]The total number of branches per 1000 carbons was determined by ^1H NMR spectroscopy. [c]Determined by GPC in trichlorobenzene at 150°C. [d]Multimodal PE distributions.

Polymerizations using **4a** in the presence of other salts such as $Cu(OSO_2CF_3)_2$, $La(OSO_2CF_3)_3$, $Ca(OSO_2CF_3)_2$, $Mg(OSO_2CF_3)_2$, and $MgCl_2$, did not appear to boost catalyst activity (Table S1). To determine whether these secondary metal salts could form adducts with **4a**, further NMR studies were conducted (Figure S20). The NMR spectra of **4a** in $CDCl_3$ were largely unaffected in the presence $La(OSO_2CF_3)_3$, $Ca(OSO_2CF_3)_2$, $Mg(OSO_2CF_3)_2$, and $MgCl_2$ (although the intensity of the triazole hydrogen peak at ~7.8 ppm was slightly decreased in the presence of $La(OSO_2CF_3)_3$ and

$Mg(OSO_2CF_3)_2$). The NMR spectrum of **4a**/Cu was significantly broadened compared to that of **4a** due to the paramagnetic copper(II). We believe that in non-coordinating solvents such as toluene and chloroform, several of these secondary metal salts are not incorporated into the nickel complexes. The use of polar co-solvents to solubilize the salts was avoided because polar solvents were found to inhibit our catalysts.

Time-Dependence Study. When we carried out a time study of ethylene polymerization by **4a**/$ZnCl_2$ (1:2), we observed that the catalyst activity gradually increased over time (Table 2, Figure 3). For example, the TOF was 263 h^{-1} after 0.5 h (Table 2, entry 5), but more than doubled to 581 h^{-1} after 3 h (entry 8). In contrast, the TOF of **4a** without zinc was nearly the same from 0 to 3 h (average TOF = 63 h^{-1}). Gel permeation chromatography (GPC) analysis of the PE products obtained using **4a**/$ZnCl_2$ (1:2) showed multimodal distributions that varied as a function of time (Figure 4).[12] GPC data deconvolution by lognormal fitting indicated that after short reaction times, from 0.5 to 1 h, mixtures containing both low (peak I, M_w = up to ~10^3) and medium molecular weight (peak II, M_w = up to ~10^4) polymers were produced. As the polymerizations proceeded from 2 to 6 h, an additional high molecular weight polymer (peak III, M_w = up to ~10^5) was observed (Figures S35–S39). Under prolonged reaction times, the PE products possessed larger amounts of higher molecular weight polymers. Polymerizations were not carried out beyond 6 h since the catalysts showed signs of decomposition. Although the M_w/M_n ratio decreased over time, the lowest polydispersity achieved was ~4.8. We attempted to access the high molecular weight generating active species directly by either 1) combining **4b**/$ZnCl_2$ for 6 h before exposing the mixture to $Ni(COD)_2$ and ethylene, or 2) combining **4b**/$ZnCl_2$/$Ni(COD)_2$ for 6 h before exposing the mixture to ethylene. Unfortunately, neither procedures yielded catalysts that showed polymerization rate enhancements or single site catalyst behavior.

Ethylene polymerization using **4b**/$ZnCl_2$ (1:2, Figures S40–S41) gave results similar to those obtained using **4a**/$ZnCl_2$. The non-uniform reactivity of the nickel-zinc complexes is unique to the heterometallic systems since catalyst **4a** itself yielded monomodal PE distributions (M_w/M_n = 1.4) regardless of the polymerization time. Although the exact nature of the nickel-zinc active species is still currently under investigation, we speculate that the coordination of Zn^{2+} to **4a** is slow and that the Cl^- anions might promote the formation of multimetallic clusters or networks.[24] It is also possible that the zinc ions could dissociate from the nickel complexes during the course of polymerization but we do not have evidence for this occurring. To probe the metal compositions and structures of the active catalysts, it is necessary to apply more advanced spectroscopic tools to monitor the polymerization reactions in situ and in real time (e.g. in operando X-ray absorption spectroscopy).[28] Such studies, however, might be complicated by the fact that these reactions generate insoluble polymers that could cause precipitation of the catalysts.

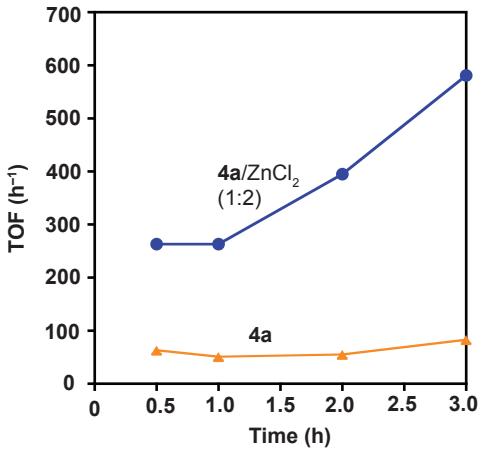

Figure 3. Comparison of the TOFs of **4a** vs. **4a**/$ZnCl_2$ (1:2).

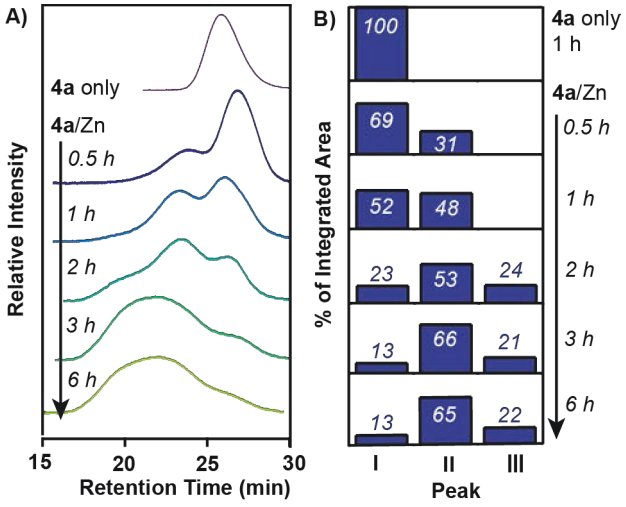

Figure 4. Plots of A) the GPC traces of PEs obtained from the reaction **4a** and **4a**/$ZnCl_2$ with ethylene; and B) the relative molecular weight distributions of the corresponding polymer samples (M_w of peak I = ~10^3, peak II = ~10^4, and peak III = ~10^5). The numbers provided in the bar graph represent percentages of the total sample. See Tables S2-S6 for more details.

CONCLUSION

In the present work, we have described our efforts to create a new family of heterometallic catalysts based on the 4-carboxamidate-1,2,3-triazole ligand system. We showed that by introducing picolyl donors to our nickel complexes, we enhanced their ability to coordinate secondary metal ions compared to our first generation catalysts. Our ethylene polymerization studies showed that the in situ formed nickel-zinc catalysts exhibited non-uniform reactivity, which most likely reflects the heterogeneous nature of their active species. One of the most important lessons from this work is that controlling the speciation of mixed-metal catalysts is not trivial since many possible metal-ligand architectures may be accessible. We propose that the picolyl group in our current catalyst design is too rotationally flexible to give heterobimetallic complexes. However, because of the modularity of our ligand construct, it should be possible to redesign the metal chelators to assemble structurally robust dinuclear catalysts in future work.

EXPERIMENTAL SECTION

General Procedures. Commercial reagents were used as received. All air- and water-sensitive manipulations were performed using standard Schlenk techniques or under a nitrogen atmosphere using a glovebox. Anhydrous solvents were obtained from an Innovative Technology solvent drying system saturated with Argon. High-purity polymer grade ethylene was obtained from Matheson TriGas without further purification. The precursor $NiBr(Ph)(PPh_3)_2$ was prepared according to a literature procedure.[23] The syntheses of ligands **3a**-**3c** are provided in the Supporting Information.

Characterization Methods. Elemental analyses were performed by Atlantic Microlab. Trace levels of solvents in elemental analysis samples were quantified by ^{1}H NMR spectroscopy. NMR spectra were acquired using JEOL spectrometers (ECA-400, 500, and 600) and referenced using residual solvent peaks. All ^{13}C NMR spectra were hydrogen atom-decoupled. ^{19}F NMR spectra were referenced to $CFCl_3$, whereas ^{31}P NMR spectra were referenced to phosphoric acid. Infrared (IR) spectra were measured using a Thermo Nicolet Avatar FT-IR spectrometer with diamond ATR. High-resolution mass spectra were obtained from the mass spectral facility at the University of Houston.

Preparation of Complex 4a. Inside the glovebox, a solution containing **3a** (100 mg, 0.28 mmol, 1.0 equiv.) and NaHMDS (76 mg, 0.41 mmol, 1.5 equiv.) in 10 mL of CH_2Cl_2 was stirred for 2 h at RT. Solid $Ni(Ph)(PPh_3)_2Br$ (204 mg, 0.28 mmol, 1.0 equiv.) was added in small portions. The reaction mixture was stirred for an additional 3 h. The resulting red mixture was filtered through a pipet plug and then dried under vacuum to give a dark red oil. Upon the addition of pentane and after stirring for ~5 min, a yellow solid formed. The product was recrystallized by dissolving in CH_2Cl_2 and then layering with pentane to afford the final product as yellow crystals (147 mg, 0.19 mmol, 69%). ^{1}H NMR ($CDCl_3$, 500 MHz): δ (ppm) = 8.56 (d, J_{HH} = 4.6 Hz, 1H), 7.84 (s, 1H), 7.61 (m, 1H), 7.44 (t, J_{HH} = 7.6 Hz, 6H), 7.32 (m, 4H), 7.18 (m, 6H), 6.85 (t, J_{HH} = 8.0 Hz, 1H), 6.80 (d, J_{HH} = 7.5 Hz, 2H), 6.56 (m, 3H), 6.24(t, J_{HH} = 7.2 Hz, 1H), 6.13 (d, J_{HH} = 7.5 Hz, 2H), 5.18 (s, 2H), 3.70 (m, 2H), 1.14 (dd, J_{HH} = 35.6 Hz, J_{HH} = 6.8 Hz, 12H). ^{13}C NMR ($CDCl_3$, 125MHz): δ (ppm) = 163.87, 152.93, 149.96, 149.52 (d, J_{CP} = 46.2 Hz), 148.89, 143.63, 142.72, 137.25, 135.59, 134.30 (d, J_{CP} = 11.2 Hz), 131.57 (d, J_{CP} = 45.0 Hz), 129.85, 127.89 (d, J_{CP} = 8.8 Hz), 125.18, 124.16, 123.77, 122.91, 122.46, 121.84, 121.11, 56.67, 29.10, 25.42, 23.26. ^{31}P NMR ($CDCl_3$, 161 MHz): δ (ppm) = 29.96. UV-vis (DCM): λ_{max}/nm (ε/cm^{-1}M^{-1}) = 331 (4559), 410 (659). FT-IR: 1597 (ν_{CO}) cm^{-1}. Mp (decomp.) = ~174°C. Anal. Calc. for $C_{45}H_{44}N_5NiOP\cdot(CH_2Cl_2)_{0.3}$: C, 69.22; H, 5.72; N, 8.91. Found: C, 69.19; H, 5.75; N, 8.91.

Preparation of Complex 4b. A similar procedure was used as described above for **4a**, except that ligand **3b** (100 mg, 0.23 mmol, 1.0 equiv.) was used instead of **3a**. Complex **4b** was obtained as a yellow solid (96.9 mg, 0.12 mmol, 51%). ^{1}H NMR ($CDCl_3$, 500 MHz): δ (ppm) = 8.56 (d, J_{HH} = 4.6 Hz, 1H), 7.84 (s, 1H), 7.61 (m, 1H), 7.44 (t, J_{HH} = 7.6 Hz, 6H), 7.32 (m, 4H), 7.18 (m, 6H), 6.85 (t, J_{HH} = 8.0 Hz, 1H), 6.80 (d, J_{HH} = 7.5 Hz, 2H), 6.56 (m, 3H), 6.24(t, J_{HH} = 7.2 Hz, 1H), 6.13 (d, J_{HH} = 7.5 Hz, 2H), 5.18 (s, 2H), 3.70 (m, 2H), 1.14 (dd, J_{HH} = 35.6 Hz, J_{HH} = 6.8 Hz, 12H). ^{13}C NMR ($CDCl_3$, 125MHz): δ (ppm) = 165.37, 152.94, 149.90, 148.62, 148.26, 143.11, 142.58, 139.63, 137.18, 135.80, 134.22 (d, J_{CP} = 10.0 Hz), 131.22 (d, J_{CP} = 46.2 Hz), 130.27, 129.92, 129.60, 127.66 (d, J_{CP} = 10.0 Hz), 127.20, 126.07, 124.88, 123.97, 123.69, 122.87, 122.22, 121.01, 56.49. ^{31}P NMR ($CDCl_3$, 161 MHz): δ (ppm) = 29.35. UV-vis (DCM): λ_{max}/nm (ε/cm^{-1}M^{-1}) = 331 (3521), 410 (659). FT-IR: 1600 (ν_{CO}) cm^{-1}. Mp (decomp.) = ~158°C. *Note: the product contained trace amounts of an impurity that could not be removed using standard purification methods.*

Preparation of Complex 4c. A similar procedure was used as described above for **4a**, except that ligand **3c** (120 mg, 0.17 mmol, 1.0 equiv.) was used instead of **3a**. Complex **4c** was obtained as a yellow solid (84.9 mg, 0.08 mmol, 45%). ^{1}H NMR ($CDCl_3$, 500 MHz): δ (ppm) = 8.53 (d, J_{HH} = 4.4 Hz, 1H), 8.10 (s, 4H), 7.91 (s, 2H), 7.84 (s, 1H), 7.58 (m, 1H), 7.25 (m, 4H), 7.02 (m, 13H), 6.29 (m, 2H), 6.13 (m, 4H), 6.12 (d, J_{HH} = 7.1 Hz, 2H), 5.10 (s, 2H). ^{13}C NMR ($CDCl_3$, 125 MHz): δ (ppm) = 166.10, 152.93, 149.82, 149.32 (d, J_{CP} = 46.2 Hz), 147.44, 144.19, 143.70, 137.08 (d, J_{CP} = 18.8 Hz), 135.21, 133.92 (d, J_{CP} = 11.2 Hz), 131.01, 130.63, 130.55, 130.48 (q, J_{CF} = 33.8 Hz), 130.39, 129.93, 127.79 (d, J_{CP} = 10.0 Hz), 125.44, 124.80, 123.86 (q, J_{CF} = 271.2 Hz), 123.62, 123.21, 121.63, 121.46, 120.06, 56.60. ^{31}P NMR ($CDCl_3$, 161 MHz): δ (ppm) = 31.29. ^{19}F NMR ($CDCl_3$, 470 MHz): δ (ppm) = -62.34. UV-vis (DCM): λ_{max}/nm (ε/cm^{-1}M^{-1}) = 331 (4058), 410 (706). FT-IR: 1605 (ν_{CO}) cm^{-1}. Mp (decomp.) = ~216°C. Anal. Calc. for $C_{55}H_{36}F_{12}N_5NiOP$: C, 60.02; H, 3.30; N, 6.36. Found: C, 59.76; H, 3.52; N, 6.39.

Ethylene Polymerization. Inside the glovebox, the nickel catalyst (25 μmol) and $ZnCl_2$ (various equiv., if any) were dissolved in 10 mL of toluene in a scintillation vial. Solid $Ni(COD)_2$ (50 μmol) was added and the solution was transferred to a Fischer-Porter glass vessel. A magnetic stir bar was placed inside and then the reactor was sealed. The high-pressure apparatus was removed from the glovebox and then securely fastened on top of a stir plate. The ethylene line was attached and the reactor was purged with ethylene three times by pressurizing with ethylene and then releasing the pressure. The reactor was then pressurized to 100 psi of ethylene and stirred at RT for a specified amount of time. The ethylene line was closed and the vessel was slowly vented. Workup procedure for isolating small amounts of polymer: About 1 mL of HCl(aq) was added to the reaction mixture, followed by the addition of 2 mL of MeOH. The aqueous layer was removed by pipetting and the organic layer was evaporated to dryness under vacuum. The resulting material was washed with MeOH and then dried under vacuum. Workup procedure for isolating large amounts of polymer: MeOH (100-200 mL) was added to precipitate the polymer from the reaction mixture. The polymer was collected by vacuum filtration, rinsed with MeOH, and dried under vacuum at 80°C overnight.

Polymer Characterization. *^{1}H NMR spectroscopy*: Each NMR sample contained ~10–20 wt% of polymer in 0.5 mL of 1,1,2,2-tetrachlorethane-d_2 (TCE-d_2) and was recorded at 500 MHz using standard acquisition parameters at 120°C. Polymer branching was calculated using the method described previously.[29]

Gel permeation chromatography (GPC): GPC analyses were performed using a Malvern high temperature GPC instrument equipped with refractive index, viscometer, and light scattering detectors. Polyethylene samples were prepared with a concentration of ~30 mg of polymer in 10 mL of solvent. The polymers were pre-dissolved in 1,2,4-trichlorobenzene

(TCB) at 150°C for at least 1 h before injection. The samples were acquired at 150°C using TCB as the mobile phase. A calibration curve was established using polystyrene standards.

Zinc Binding Studies by NMR Spectroscopy. Complex **4a**-**4c** (5 mg) and $ZnCl_2$ (0–10 equiv., relative to Ni) were combined in 0.5 mL of chloroform-*d*. The mixtures were sonicated until most of the zinc salt had dissolved. These samples were then transferred to NMR tubes and their ^1H NMR spectra were recorded at various temperatures.

Zinc Binding Studies by UV-Vis Absorption Spectroscopy. A stock solution of **4a (**100 μM) was prepared by dissolving 10 μmol of **4a** in 100 mL of dichloromethane and a stock solution of $ZnCl_2$ (30 mM) was prepared by dissolving 0.3 mmol of $ZnCl_2$ in 10 mL of EtOH. A 3.0 mL solution of **4a** was transferred to a 1 cm quartz cuvette and then sealed with a septum screw cap. The cuvette was placed inside a UV-vis spectrophotometer and the spectrum of **4a** was recorded. Aliquots containing 1 equiv. of $ZnCl_2$ (10 μL), relative to **4a**, were added using a micropipetter and the solution was shaken for 2 min before the spectra were measured. The titration studies were stopped after the addition of up to 10 equiv. of $ZnCl_2$.

ASSOCIATED CONTENT

Supporting Information

The Supporting Information is available free of charge on the ACS Publications website.

Synthetic procedures, NMR spectra, and X-ray data (PDF).

AUTHOR INFORMATION

Corresponding Author

*loido@uh.edu

Notes

The authors declare no competing financial interest.

ACKNOWLEDGMENT

We thank the Welch Foundation (Grant No. E-1894), ACS Petroleum Research Fund (Grant No. 54834-DNI3), and the National Science Foundation (CHE-1750411) for funding this work. We are grateful to Hsin-Chun (Jimmy) Chiu (University of Minnesota) for help with GPC data deconvolution.

REFERENCES

(1) Lin, Y.-W. Rational Design of Metalloenzymes: From Single to Multiple Active Sites. *Coord. Chem. Rev.* **2017**, *336*, 1-27.

(2) Delferro, M.; Marks, T. J. Multinuclear Olefin Polymerization Catalysts. *Chem. Rev.* **2011**, *111*, 2450-2485.

(3) Carrow, B. P.; Nozaki, K. Transition-Metal-Catalyzed Functional Polyolefin Synthesis: Effecting Control Through Chelating Ancillary Ligand Design and Mechanistic Insights. *Macromolecules* **2014**, *47*, 2541-2555.

(4) Jüngling, S.; Müllhaupt, R.; Plenio, H. Cooperative Effects in Binuclear Zirconocenes: Their Synthesis and Use As Catalyst in Propene Polymerization. *J. Organomet. Chem.* **1993**, *460*, 191-195.

(5) Suo, H.; Solan, G. A.; Ma, Y.; Sun, W.-H. Developments in Compartmentalized Bimetallic Transition Metal Ethylene Polymerization Catalysts. *Coord. Chem. Rev.* **2018**, *372*, 101-116.

(6) Takano, S.; Takeuchi, D.; Osakada, K.; Akamatsu, N.; Shishido, A. Dipalladium Catalyst for Olefin Polymerization: Introduction of Acrylate Units into the Main Chain of Branched Polyethylene. *Angew. Chem., Int. Ed. Engl.* **2014**, *53*, 9246-9250.

(7) Radlauer, M. R.; Buckley, A. K.; Henling, L. M.; Agapie, T. Bimetallic Coordination Insertion Polymerization of Unprotected Polar Monomers: Copolymerization of Amino Olefins and Ethylene by Dinickel Bisphenoxyiminato Catalysts. *J. Am. Chem. Soc.* **2013**, *135*, 3784-3787.

(8) Cai, Z.; Xiao, D.; Do, L. H. Fine-Tuning Nickel Phenoxyimine Olefin Polymerization Catalysts: Performance Boosting by Alkali Cations. *J. Am. Chem. Soc.* **2015**, *137*, 15501-15510.

(9) Cai, Z.; Do, L. H. Customizing Polyolefin Morphology by Selective Pairing of Alkali Ions with Nickel Phenoxyimine-Polyethylene Glycol Catalysts. *Organometallics* **2017**, *36*, 4691-4698.

(10) Johnson, L.; Wang, L.; McLain, S.; Bennett, A.; Dobbs, K.; Hauptman, E.; Ionkin, A.; Ittel, S.; Kunitsky, K.; Marshall, W.; McCord, E.; Radzewich, C.; Rinehart, A.; Sweetman, K. J.; Wang, Y.; Yin, Z.; Brookhart, M. Copolymerization of Ethylene and Acrylates by Nickel Catalysts. In *Beyond Metallocenes*; American Chemical Society: 2003; Vol. 857, p 131-142.

(11) Kuwabara, J.; Takeuchi, D.; Osakada, K. Early-Late Heterobimetallic Complexes As Initiator for Ethylene Polymerization. Cooperative Effect of Two Metal Centers to Afford Highly Branched Polyethylene. *Chem. Commun.* **2006**, 3815-3817.

(12) Chiu, H.-C.; Koley, A.; Dunn, P. L.; Hue, R. J.; Tonks, I. A. Ethylene Polymerization Catalyzed by Bridging Ni/Zn Heterobimetallics. *Dalton Trans.* **2017**, *46*, 5513-5517.

(13) Mankad, N. P. Non-Precious Metal Catalysts for C–H Borylation Enabled by Metal–Metal Cooperativity. *Synlett* **2014**, *25*, 1197-1201.

(14) Cooper, B. G.; Napoline, J. W.; Thomas, C. M. Catalytic Applications of Early/Late Heterobimetallic Complexes. *Cat. Rev.* **2012**, *54*, 1-40.

(15) Ritleng, V.; Chetcuti, M. J. Hydrocarbyl Ligand Transformations on Heterobimetallic Complexes. *Chem. Rev.* **2007**, *107*, 797-858.

(16) Shibasak, i. M.; Kanai, M.; Matsunaga, S.; Kumagai, N. Multimetallic Multifunctional Catalysts for Asymmetric Reactions. In *Bifunctional Molecular Catalysis. Topics in Organometallic Chemistry*; Ikariya, T., Shibasaki, M., Eds.; Springer: Berlin, Heidelberg, 2011; Vol. 37, p 1-30.

(17) Chen, E. Y.-X. Coordination Polymerization of Polar Vinyl Monomers by Single-Site Metal Catalysts. *Chem. Rev.* **2009**, *109*, 5157-5214.

(18) Nakamura, A.; Ito, S.; Nozaki, K. Coordination-Insertion Copolymerization of Fundamental Polar Monomers. *Chem. Rev.* **2009**, *109*, 5215-5244.

(19) Ittel, S. D.; Johnson, L. K.; Brookhart, M. Late-Metal Catalysts for Ethylene Homo- and Copolymerization. *Chem. Rev.* **2000**, *100*, 1169-1203.

(20) Xiao, D.; Do, L. H. Triazolecarboxamidate Donors as Supporting Ligands for Nickel Olefin Polymerization Catalysts. *Organometallics* **2018**, *37*, 254-260.

(21) Mindt, T. L.; Schibli, R. Cu(I)-Catalyzed Intramolecular Cyclization of Alkynoic Acids in Aqueous Media: A "Click Side Reaction". *J. Org. Chem.* **2007**, *72*, 10247-10250.

(22) Ditri, T. B.; Carpenter, A. E.; Ripatti, D. S.; Moore, C. E.; Rheingold, A. L.; Figueroa, J. S. Chloro- and Trifluoromethyl-Substituted Flanking-Ring m-Terphenyl Isocyanides: η-Arene Binding to Zero-Valent Molybdenum Centers and Comparison to Alkyl-Substituted Derivatives. *Inorg. Chem.* **2013**, *52*, 13216-13229.

(23) Standley, E. A.; Smith, S. J.; Müller, P.; Jamison, T. F. A Broadly Applicable Strategy for Entry into Homogeneous Nickel(0) Catalysts from Air-Stable Nickel(II) Complexes. *Organometallics* **2014**, *33*, 2012-2018.

(24) Bai, S.-Q.; Jiang, L.; Sun, B.; Young, D. J.; Hor, T. S. A. Five Cu(II) and Zn(II) Clusters and Coordination Polymers of 2-Pyridyl-1,2,3-triazoles: Synthesis, Structures and Luminescence Properties. *CrystEngComm* **2015**, *17*, 3305-3311.

(25) Mu, H.; Pan, L.; Song, D.; Li, Y. Neutral Nickel Catalysts for Olefin Homo- and Copolymerization: Relationships Between Catalyst Structures and Catalytic Properties. *Chem. Rev.* **2015**, *115*, 12091-12137.

(26) Valente, A.; Mortreux, A.; Visseaux, M.; Zinck, P. Coordinative Chain Transfer Polymerization. *Chem. Rev.* **2013**, *113*, 3836-3857.
(27) van Meurs, M.; Britovsek, G. J. P.; Gibson, V. C.; Cohen, S. A. Polyethylene Chain Growth on Zinc Catalyzed by Olefin Polymerization Catalysts: A Comparative Investigation of Highly Active Catalyst Systems across the Transition Series. *J. Am. Chem. Soc.* **2005**, *127*, 9913-9923.
(28) Fabbri, E.; Abbott, D. F.; Nachtegaal, M.; Schmidt, T. J. Operando X-ray Absorption Spectroscopy: A Powerful Tool Toward Water Splitting Catalyst Development. *Curr. Opin. Electrochem.* **2017**, *5*, 20-26.
(29) Wiedemann, T.; Voit, G.; Tchernook, A.; Roesle, P.; Göttker-Schnetmann, I.; Mecking, S. Monofunctional Hyperbranched Ethylene Oligomers. *J. Am. Chem. Soc.* **2014**, *136*, 2078-2085.

Table of Contents